# Global Sensitivity Analysis of 0-D Lithium Sulfur Electrochemical Model

Chitra Dangwal, Dylan Kato, Zhijia Huang, Aaron Kandel, Scott Moura\*

\* University of California, Berkeley, Berkeley, CA 94720 USA (e-mail: chitra\_dangwal@berkeley.edu, dkkato@berkeley.edu, hzj19@berkeley.edu, akandel@berkeley.edu, smoura@berkeley.edu)

#### Abstract:

This paper examines global parameter sensitivity in a zero-dimensional lithium-sulfur (Li-S) battery model. Li-S batteries are an appealing cell chemistry due to their high theoretical energy density, abundant supply, and low cost. However, due to the lack of complete understanding of the underlying working mechanisms for Li-S cells, the development of mathematical models and state estimation is still at its early stages. Model development and parameter identification are closely associated. Both are essential for developing battery management systems (BMS) in commercialized Li-S powered applications. This paper highlights the parameter identification challenges associated with Li-S models. Sensitivity analysis helps for parameter identification by revealing information about parameter relevance and interdependence. Sensitivity analysis also helps in understanding different physical ranges of parameters, and their impact on model performance/response. In this work we examine global sensitivity analysis (GSA). A key challenge for GSA, especially in Li-S batteries, is a lack of available information in the literature about a-priori distributions of Li-S parameters. This paper aims to elucidate this challenge by comparing GSA under different parameter distributions. Three model parameters are chosen in this analysis, and their sensitivities are compared under three different distributions. We find that, under certain distributions of parameters, relative importance of the parameters shifts.

Keywords: Lithium-Sulfur Battery, Global Sensitivity Analysis, Sensitivity Analysis, Parameter, Sobol Indicies, Identification

# 1. INTRODUCTION

With an increasing push for electrification, research on higher energy density battery chemistry has gained momentum, especially in applications where energy density is critically important. Research on Lithium sulfur batteries has gained traction due to their high theoretical energy density 2500  $\mathrm{Wh\cdot kg^{-1}}$  (Guo et al. (2017)). The practical energy density is expected to be 2-3 times greater than current Li-ion batteries (Parke et al. (2021), Fotouhi et al. (2017)). The abundant supply and low cost of sulfur adds to the commercial interest in Li-S batteries. Consequently, recent years have shown accelerated research in different areas for Li-S, from understanding fundamental reaction mechanisms, suitable electrolyte/electrode design, modelling and controls (Lim et al. (2019), Peng et al. (2020)). Even though the chemistry is promising due to higher energy densities, its commercialization is hindered by the limited utilization of sulfur, poor rate capability, selfdischarge, and capacity degradation. Shuttling of soluble polysulfides during cycling between the cathode and anode acts as a parasitic side reaction, causes formation of Li<sub>2</sub>S layer on the Li anode, thus causing capacity fade and low cyclic efficiency (Feng et al. (2022), Liu et al. (2018)). This

shuttle effect is blamed as a major hindrance toward the commercialization of Li-S batteries.

There are a lot of efforts focused on mitigating the shuttle effect, improving cell chemistry, and electrolyte design. Most of the research on Li-S batteries focuses on materials (Lim et al. (2019)), chemical development (Hou et al. (2017)), and understanding the reaction fundamentals of the battery (Peng et al. (2020)), which are all essential to its development (Feng et al. (2022)). Nonetheless, it is also essential to develop BMS systems based on mathematical models, including state and parameter estimation algorithms that monitor performance and health (Fotouhi et al. (2017)).

Depending on the physical scales, Li-S models in literature range from, atomic level DFT simulations, to microparticle level kinetics, to bulk macroscale cell-level models to system level models (Hou et al. (2015), Wang et al. (2021), Kumaresan et al. (2008), Marinescu et al. (2016)). The lower the magnitude of physical range of model, the higher the model complexity gets due to inclusion of more fundamental interactions (e.g. absorption energies, molecular transport). A key aspect in model development is identification of model parameters to align the model prediction to experimental data (Parke et al. (2021)). In case of Li-S, complex reaction mechanisms make both modeling and parameter identification a daunting challenge. Mathematical models with large number of parameters are

 $<sup>^\</sup>star$  Sponsor and financial support acknowledgment goes here. Paper titles should be written in uppercase and lowercase letters, not all uppercase.

# CONFIDENTIAL. Limited circulation. For review only.

generally associated with more complex parameter identification. In this regard, efforts are made on reducing model complexity, experimental identification of parameters and investigating parameter sensitivities.

Sensitivity analysis uncovers the effect of parameters on model response. It guides parameter identification by revealing information about parameter relevance and interdependence, which helps in grouping and ordering the parameters during the identification process (Park et al. (2018)). It also helps in optimally designing experiments such that these parameters can be measured/estimated under ordinary non-destructive testing conditions. The literature on parameter sensitivity and identification for Li-S battery is limited. (Xu et al. (2021)) in their study investigated parameter sensitivity for 0-D Li-S model, to identify significant parameters for parameter identification. In their study, they compared the performance of four 0-D models with different reaction mechanisms, w.r.t. fitting to experimental discharge data. The authors in this work use local sensitivity analysis which is computed by the derivative of voltage with respect to the varied parameter. Important parameters are identified by sensitivity analyses which then used in their identification. A key challenge in this work is that the 'nominal' parameter values are unknown, thus, local sensitivity analysis suffers from a chicken and egg problem, where to identify the parameters you must use a tool which assumes you know the parameter values. This motivates the use of Global sensitivity techniques which don't assume initial point estimates on parameters and instead only assume the parameters live in a range of values.

Ghaznavi and Chen in a series of three papers, explore the sensitivity of parameters for a 1-D electrochemical model (Kumaresan et al. (2008)) at different set values of parameters. In their first work (Ghaznavi and Chen (2014b)), they studied the cell performance for a wide range of discharge current rates and cathode conductivity. They found that cell capacity performance for high current rate was limited because of sulfur dissolution in electrolyte. They also found a lower limit in conductivity below which the cell ceases to operate. In their second work (Ghaznavi and Chen (2014b)), the discharge behavior was studied under a range of values of precipitation rate constants. By doing so they uncovered the role of sulfur dissolution and precipitation on capacity performance. They further proposed an optimal sulfur content for higher capacity performance. In their third work (Ghaznavi and Chen (2014a)) they investigated the effect of exchange current densities and the diffusion coefficients on reaction kinetics and transport process. Relative magnitude of exchange current densities help in illuminating the dominant and rate limiting reaction. The study performed in (Ghaznavi and Chen (2014a)) can be used to optimally design the cell in relation to influence of parameter on cell performance. The parameter sampling technique in these works faces two major challenges. First, the parameters are varied one at a time and therefore do not capture the effect of parameter interaction on the output. Second, the parameters are sampled form an assumed set, which does not necessarily signify actual physical values of parameters. This motivates using techniques that explore the interaction of

parameters and systematic sampling of parameter values, such as global sensitivity analysis.

In (Parke et al. (2020)) the authors developed a Tankin-Series model as an equivalent 1-D Li-S electrochemical model. The authors study parameter sensitivities of the model's diffusion coefficients and cathode thickness for different current rates to check the suitability of the model. Similar to (Kumaresan et al. (2008)), sensitivity of parameters is evaluated by analysing the model response at different set values of parameters. Choosing parameters in this way can be insightful, however it is inherently heuristic in nature and does not systematically capture how the range of these set points affect the voltage response.

Senstivity analysis methods are generally classified into two categories: local sensitivity analysis (LSA) and GSA. The two methods are different from each other in the kind of information they represent. LSA evaluates first order derivatives at a specific reference point in the parameter space. Therefore, changing the 'reference point' changes the information obtained from LSA. Despite being reference point dependent, LSA is used extensively in the literature (Park et al. (2018), Xu et al. (2021)) because it provides qualitative, easily interpretable information which is also computationally cheap to evaluate.

On the other hand, GSA measures the magnitude of influence a parameter has on model response. It is global in the sense that it evaluates the sensitivity over a given probability distribution on the parameter (Ramancha et al. (2022)). Even though GSA is considered 'global', as a range of parameters are considered in calculating sensitives, the sensitivities obtained depend on the choice of parameter distribution (Saltelli et al. (2008)). The downside of using GSA is related computational cost, which increases exponentially as the number of parameters in the analysis increases.

Generally, GSA is thought to be advantageous with respect to LSA because it more effectively captures the range in which parameters may exist. However, even in the GSA case, we rely on good estimates of the parameter distribution to understands the relative parameter importance.

To address this challenge, we conduct a meta-sensitivity analysis on GSA under 3 parameter distributions to understand the way GSA sensitivities change as you change the parameter distribution. To this end, we perform sensitivity analysis on a 0-D electrochemical Li-S model (Huang et al.). A global sensitivity evaluation method, i.e. Sobol index (Saltelli et al. (2010)) is used for analyzing parameter sensitivities. We use GSA in this study, firstly due to lack of experimentally validated nominal values of parameters (Parke et al. (2021)) and also to explore the interaction effect of parameters. It is recognized that lack of definitive possible physical values is a problem that Li-S models face. To this extent, we performed sensitivity analysis for three different distributions of model parameters. This is done to examine the effect information about parameter a-priori have on its relative importance in parameter identification. To simplify, we focus on 3 of the model parameters for performing sensitivity analysis. This study is performed on 2 current profiles, to also emphasis the importance of experimental design on parameter identification. The main contributions of this paper are thus:

- (1) Analysis of a 0D lithium Sulfur battery model using global sensitivity analysis.
- (2) Analysis of Global sensitivity methods and their robustness to parameter distributions. To the authors knowledge, this is the first work that explores how parameter distributions change the results of global sensitivity analysis.

The paper is organized as follows. Section 2 introduces the zero-dimensional electrochemical model considered in the study. Section 3 details the global sensitivity technique used for performing sensitivity analysis and details the different parameter distributions chosen in the study. Section 4 outlines the implementation of GSA. Section 5 presents the results of sensitivity analysis and details the comparative sensitivity analysis of different parameter distributions. Finally, section 6 provides conclusion for the overall study.

### 2. LI-S BATTERY MODEL

This section summarizes a macro level electrochemical model, i.e. the zero-dimensional Li-S model, developed in the previous work (Huang et al.). The model captures the fundamental redox reaction mechanisms happening at the cathode, while disregarding the diffusion related transport phenomena. This model only considers the reaction kinetics on the cathode side. The reaction kinetics/ overpotential losses at the anode side are neglected. The anode is taken as Li metal, which is assumed to be an unlimited source of Li.

During discharge the Li-metal anode goes through an oxidation reaction, liberating Li-ions. The Li-ions move across the electrolyte towards the cathode, where they react with the sulfur species and gets reduced into different Li-polysulfide species. At the cathode, the elemental sulfur  $S_8^0$  undergoes a series of complex electrochemical reactions, forming different polysulfide species  $\text{Li}_2S_n$  (1 \le n \le 8), starting from high order polysufides and finally reducing to low order sulfide Li<sub>2</sub>S. The high order polysufides are soluble in organic electrolytes, which causes shuttling of the high order sulfide species between cathode and anode. This parasitic 'shuttle' effect causes self-discharge and degradation of the anode.

The zero-dimensional model chosen for this study is a 3step electrochemical reaction given by:

$$\frac{3}{8}S_8^0 + e^- \longleftrightarrow \frac{1}{2}S_6^{2-},\tag{1}$$

$$S_6^{2-} + e^- \longleftrightarrow \frac{3}{2}S_4^{2-}, \tag{2}$$

$$\frac{1}{6}S_4^{2-} + e^- \longleftrightarrow \frac{2}{3}S^{2-} \downarrow . \tag{3}$$

The lowest polysulfide i.e.,  $S^{2-}$  further principates. A schematic of the reaction pathway during discharge is shown in Fig. 1.

The mass evolution of sulfur species is described by the following equations (4) -(8):

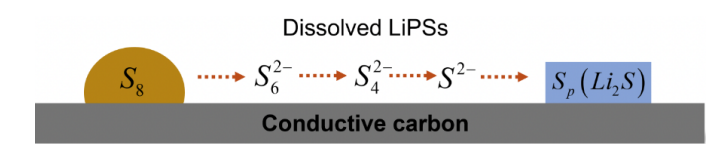


Fig. 1. A schematic of the reaction pathway during discharge at the cathode (Huang et al.)

$$\dot{x}_1 = -\frac{3}{8} \frac{n_{\rm S8} M_{\rm S}}{n_{\rm e} F} i_{H1} - k_s x_1,\tag{4}$$

$$\dot{x}_2 = \frac{1}{2} \frac{n_{S6} M_S}{n_e F} i_{H1} - k_s x_2 - \frac{n_{S6} M_S}{n_e F} i_{H2}, \tag{5}$$

$$\dot{x}_3 = \frac{3}{2} \frac{n_{\rm S4} M_{\rm S}}{n_e F} i_{H2} - \frac{1}{6} \frac{n_{\rm S4} M_{\rm S}}{n_e F} i_L, \tag{6}$$

$$\dot{x}_4 = \frac{2}{3} \frac{n_e F}{n_e F} i_L - k_p x_5 (x_4 - S_*^{2-}), \tag{7}$$

$$\dot{x}_7 = k_c x_7 (x_7 - S_*^{2-}) \tag{8}$$

$$\dot{x}_5 = k_p x_5 (x_4 - S_*^{2-}). (8)$$

where states  $[x_1, x_2, x_3, x_4, x_5]$  represent the mass of sulfur species  $[S_8^0, S_6^{2-}, S_4^{2-}, S^{2-}, S_p]$  respectively. The shuttling effect of high order polysulfides i.e.  $S_8^0$  and  $S_6^{2-}$  is modeled by using a shuttling constant  $k_s$ . The precipitation of  $S^{2-}$  is modeled using equation with a precipitation rate constant  $k_n$ .

The standard reduction potentials associated with the 3 reactions (1)-(3) can be modeled using Nernst equation given by equations (9)-(11).

$$E_{H1} = E_{H1}^{0} - \frac{RT}{F} \left( -\frac{3}{8} \ln \left( \frac{x_1}{n_S M_S v} \right) + \frac{1}{2} \ln \left( \frac{x_2}{n_{S6} M_S v} \right) \right), \tag{9}$$

$$E_{H2} = E_{H2}^{0} - \frac{RT}{F} \left( -\ln\left(\frac{x_2}{n_{S6}M_S v}\right) + \frac{3}{2}\ln\left(\frac{x_3}{n_{S4}M_S v}\right) \right), \tag{10}$$

$$E_L = E_L^0 - \frac{RT}{F} \left( -\frac{1}{6} \ln \left( \frac{x_3}{n_{S4} M_{S} v} \right) + \frac{2}{3} \ln \left( \frac{x_4}{n_{S} M_{S} v} \right) \right). \tag{11}$$

The current associated with the 3 reactions (1)-(3) is modeled by using Butler-Volmer equations (12)-(14).

$$i_{H1} = -i_{H1}^{0} a_{r} \cdot \left[ \left( \frac{x_{1}}{x_{1}^{0}} \right)^{-\frac{3}{8}} \left( \frac{x_{2}}{x_{2}^{0}} \right)^{\frac{1}{2}} e^{\frac{F\eta_{H1}}{2RT}} - \left( \frac{x_{1}}{x_{1}^{0}} \right)^{\frac{3}{8}} \left( \frac{x_{2}}{x_{2}^{0}} \right)^{-\frac{1}{2}} e^{-\frac{F\eta_{H1}}{2RT}} \right]$$

$$(12)$$

$$i_{H2} = -i_{H2}^{0} a_{r} \cdot \left[ \left( \frac{x_{2}}{x_{2}^{0}} \right)^{-1} \left( \frac{x_{3}}{x_{3}^{0}} \right)^{\frac{3}{2}} e^{\frac{F\eta_{H2}}{2RT}} - \left( \frac{x_{2}}{x_{2}^{0}} \right) \left( \frac{x_{3}}{x_{3}^{0}} \right)^{-\frac{3}{2}} e^{-\frac{F\eta_{H2}}{2RT}} \right]$$

$$(13)$$

$$i_{L} = -i_{L}^{0} a_{r} \cdot \left[ \left( \frac{x_{3}}{x_{3}^{0}} \right)^{-\frac{1}{6}} \left( \frac{x_{4}}{x_{4}^{0}} \right)^{\frac{2}{3}} e^{\frac{F\eta_{L}}{2RT}} - \left( \frac{x_{3}}{x_{3}^{0}} \right)^{\frac{1}{6}} \left( \frac{x_{4}}{x_{4}^{0}} \right)^{-\frac{2}{3}} e^{-\frac{F\eta_{L}}{2RT}} \right]$$

$$(14)$$

The total current flowing in the battery is the sum of the current across the three reactions.

$$I = i_{H1} + i_{H2} + i_L. (15)$$

The precipitation of sulfide  $S_p$ , causes loss of active reaction area which is modeled as:

$$a_r = a_r^0 (1 - \omega \cdot x_5)^{\gamma}. \tag{16}$$

The overall output voltage is related to the standard reduction potential and overpotential of the three reactions.

$$\eta_{H1} = V - E_{H1},\tag{17}$$

$$\eta_{H2} = V - E_{H2},$$
 $\eta_{L} = V - E_{L}.$ 
(18)

$$\eta_L = V - E_L. \tag{19}$$

The equations above collectively form a differential algebraic equation (DAE) model whose parameters are summarized in Table 1.

Table 1. Zero-Dimensional Model Notation

Notation	Name	Units
$M_{ m S}$	Molar mass of S	[g/mol]
$n_{\rm S8}, n_{\rm S6}, n_{\rm S4}, n_{\rm S}$	No. of S atoms in polysulfide	[-]
$n_e$	No. of electron per reaction	[-]
F	Faraday's constant	[C/mol]
R	Gas constant	[J/K/mol]
T	Temperature	[K]
$k_s$	Shuttle constant	$[s^{-1}]$
$k_p$	Precipitation rate	$[s^{-1}]$
$S^{oldsymbol{k_p}}_*$	$S^{2-}$ Saturation mass	[g]
$E_{H_1}^0$	Standard potential, rxn 1	[V]
$E_{H2}^{0}$	Standard potential, rxn 2	[V]
$E_L^{0}$	Standard potential for rxn 3	[V]
$egin{array}{c} i_{H1}^0 \ i_{H2}^0 \end{array}$	Exchange current density, rxn 1	$[A/m^2]$
$i_{H2}^{0}$	Exchange current density, rxn 2	$[A/m^2]$
$i_{L,0}$	Exchange current density, rxn 3	$[A/m^2]$
$x_j^0 \ I$	Initial mass of species $j$	[g]
$ec{I}$	Applied current	[A]
$a_r$	Active reaction area	$[m^2]$
$a_r^0$	Initial active reaction area	$[m^2]$
$\gamma$	Power of the relative porosity	[-]
$\omega$	Relative porosity change rate	[1/g]
v	Electrolyte volume per cell	[L]
$\eta_{H1}, \eta_{H2}, \eta_{L}$	Surface overpotentials	[V]

### 3. PARAMETER SENSITIVITY

This section focuses on the parameter sensitivity information evaluated from GSA, for different parametric distributions.

In the 0-D model considered in this study, there are 11 model parameters in total. In this study we focus on 3 parameters due of the constraints on computational time required for GSA calculations. The parameters considered in the sensitivity analysis are:  $E_{H01}$ ,  $i_{H01}$  and  $k_p$ . These 3 parameters are chosen in this study, as ranges of their respective distribution can vary significantly. This makes the analysis on the effect of parameter distribution in GSA interesting.

# 3.1 Global Sensitivity Analysis

GSA quantifies the variation of model response by varying the parameters along the entire parameter domain. A variance-based GSA tool, i.e. Sobol index, is used in this study (Saltelli et al. (2010)). The Sobol index, is a measure of the percentage of variance in model output, caused

by a particular parameter or its interaction with other parameters. The variance in model output as a function of its parameter is decomposed as:

$$\operatorname{var}(y(p)) = \sum_{i=1}^{n_p} \operatorname{var}(y_i(p_i)) + \sum_{i < j}^{n_p} \operatorname{var}(y_{ij}(p_i, p_j)) + \cdots + \operatorname{var}(y_{1,2,\dots,n_p}(p_1, p_2, \dots, p_{n_p}))$$
(20)

where y is the model output  $p_i$  is the  $i^{th}$  model parameter and  $n_p$  is the number of parameters in the model. Each term in the distribution above is orthogonal and is based on the assumption of independence of model parameters. Next we define each term.

The first term in the decomposition represents the output variance caused by parameter  $p_i$  alone and is calculated

$$\operatorname{var}(y_i(p_i)) = \operatorname{var}_{p_i} \left( \underset{p_{\sim i}}{\mathbb{E}} (y \mid p_i) \right)$$
 (21)

where the conditional expectation is taken over the joint distribution of random vector p, marginalized with respect to parameter i, and given  $p_i$ .

The second and the following terms capture the effect of varying parameters simultaneously, and are called second order interactions, and corresponding higher order interactions. The 2nd order interaction terms are calculated as follows:

$$\operatorname{var}(y_{ij}(p_i, p_j)) = \operatorname{var}_{p_i, p_j} \left( \underset{p_{\sim ij}}{\mathbb{E}} (y \mid p_i, p_j) \right) - \operatorname{var}(y_i(p_i)) - \operatorname{var}(y_j(p_j))$$
(22)

These decomposed partial variances are normalized w.r.t. the total variance and is termed as the corresponding Sobol index. The commonly used Sobol indices are:

- (1) First-order indices:  $S_{1,i} = \text{var}(y_i(p_i))/\text{var}(y)$
- (2) Second-order indices:  $S_{2,ij} = \text{var}(y_{ij}(p_i, p_j))/\text{var}(y)$ (3) Total-order index:  $S_{T,i} = S_i + S_{ij} + S_{ijk} + \ldots + S_{1,\ldots,n_p}$

In this study we use the Sobol index framework for analyzing global sensitivities of the 3 parameters  $E_{H1}^0, i_{H1}^0$ and  $k_p$ .

# 4. MONTE CARLO IMPLEMENTATION

To compute the Sobol indices we conduct a Monte Carlo analysis. We use CasADi (Andersson et al. (2019)) to simulate the model and voltage response for parameters sampled randomly from the three distributions. We then use the package SALib (Iwanaga et al. (2022)) to compute Sobol indices over these simulations. We run 512 Monte Carlo simulations for each parameter distribution.

We analyze the global sensitives under 3 different parametric distribution as shown in Table 2.

Table 2. Distribution of parameters

Param.	Distribution 1	Distribution 2	Distribution 3
$E_{H1}^0$	5% (Uniform)	5% (Uniform)	5% (Uniform)
$i_{H1}^0$	5% (Uniform)	20% (Uniform)	1 order (Log-norm)
$k_p$	5% (Uniform)	20% (Uniform)	2 order (Log-norm)

The parameter distributions analyzed is either a uniform or a lognormal around a nominal value. All three distribution sets consider a 5% variation in  $E_{H1}^0$ , since the

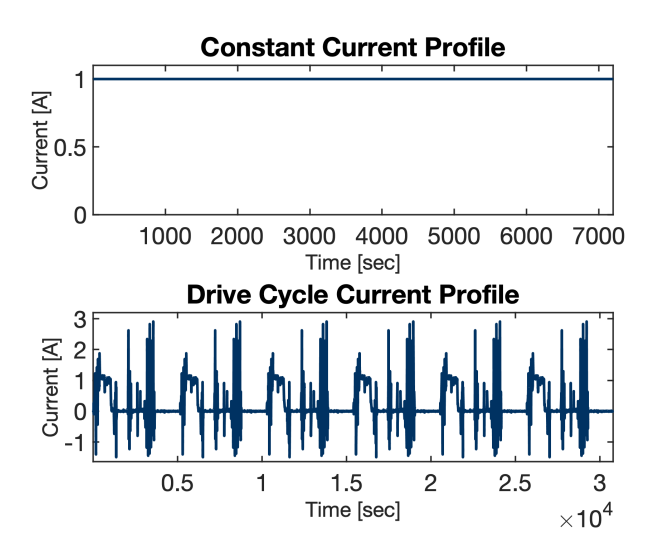


Fig. 2. Input current profiles

standard reduction potential can generally only vary by 0.5 V. The other parameters  $i_{H1}^0$  and  $k_p$ , however, do not have a defined nominal range of values. In literature, the estimated values of these parameters vary significantly by 1 or 2 orders of magnitude (Xu et al. (2021), Marinescu et al. (2016)). Hence these 3 parameter distribution sets are considered in the analysis, with different degrees of parametric variation.

### 5. RESULTS

In this section we analyze the results of GSA for the following input profiles:

- 1A constant current (C/3) discharge
- A dynamic current input

For each current profile, we show the GSA results for the selected 3 model parameters  $\{E_{H01},\ i_{H01},\ k_p\}$  and 3 probability distributions on those parameters. For each parameter distribution set (Table 2), we also analyze the resulting distribution on the state trajectory. We use first order Sobol indices as a measure of parameter sensitives. We find that, for certain parameters, the first-order Sobol indicies are strongly impacted by the parameter distribution.

### 5.1 Constant Current Analysis

Figure 3 shows the model voltage distribution for the constant current input for 3 different distributions. Each of the three subplots represents a different parameter distribution. The blue and yellow lines in the figure represent the mean voltage response and its corresponding plus/minus one standard deviation, respectively, for each distribution. We observe that voltage variance is large in the first 3000 seconds for all distribution sets, and distribution set 3 uniquely shows higher variation after 4500 second. The model remains relatively insensitive between 3500-4500 seconds across all three parameter distributions.

Sobol indicies for the constant current input are shown in Fig 4. It can be observed that for all the distributions, parameter  $E_{H1}^0$  remains sensitive in the initial 4000 seconds,

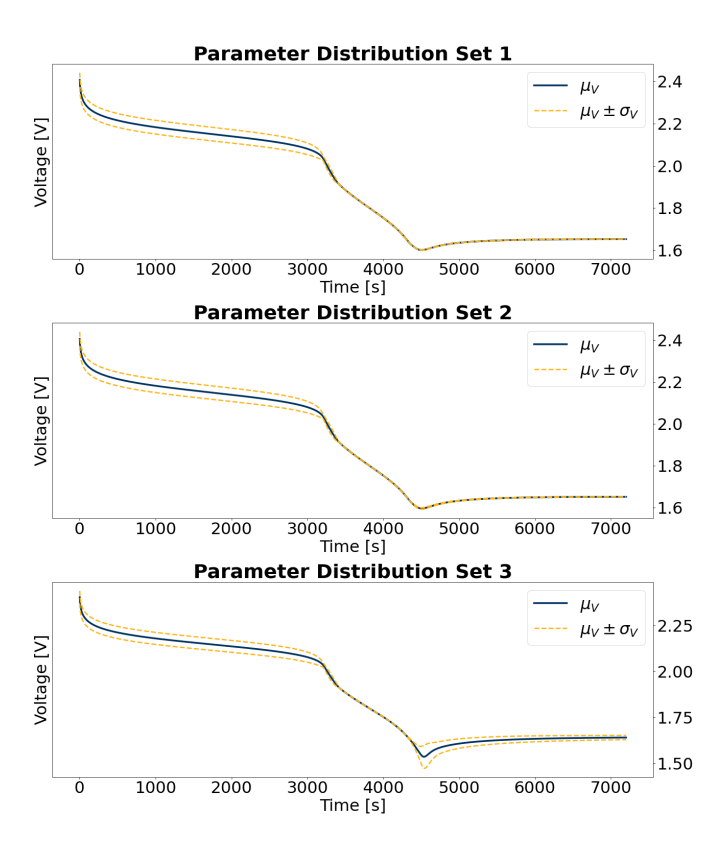


Fig. 3. Voltage response for the 3 parameter distribution sets at constant current

while parameter  $k_p$  only becomes significant in the latter part of the profile. It is also interesting to observe the parameter  $i_{H1}^0$  has very low sensitivity for distribution set 1 and 2, while for distribution set 3 its sensitivity increases.

The explanation for greater variance for distribution set 3 after 4500 seconds, and corresponding sensitivity profiles, can be inferred by analyzing the state evolution of sulfur species (Fig. 5). The figure shows the evolution of sulfur species for 1A constant current for the three parameter distributions.

Table 3. Normalizing constants for state plots

States	Constant Current	Drive cycle Current
$x_1$	2.97	2.97
$x_2$	2.54	2.38
$x_3$	2.95	1.24
$x_4$	0.027	4.46e-05
$x_5$	0.604	3e-05

The solid and the dotted lines in the figure, denote mean and min/max evolution of the sulfur species using the parameters from the three distributions. It should be noted that the plots of species in the figure are normalized by maximum of each state over all three distributions. These normalizing constants are shown in table 3. It can be observed that species  $S_8$  and  $S_6$ , which are affected by parameters  $E_{H1}^0$  and  $i_{H1}^0$  according to equations (9) and (12), are only present in the initial 4000 secs. Once  $S_8$  is exhausted around 3000 sec and  $S_6$  starts decreasing, the variance caused by parameter  $E_{H1}^0$  on model output decreases significantly. As  $S_8$  is depleted, reaction 1 is no longer a prevalent reaction, thereby equations (9) and (12) cease to affect voltage output.

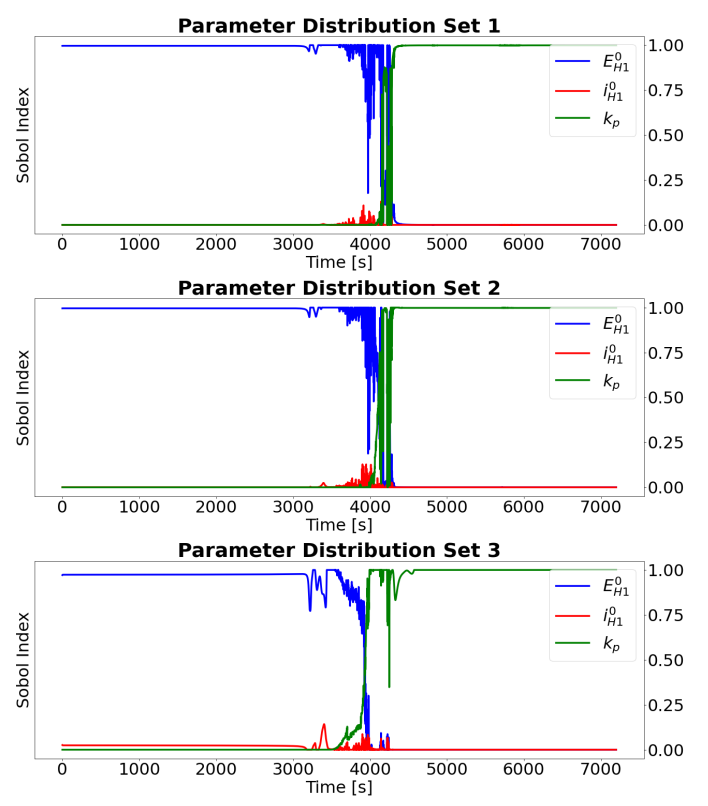


Fig. 4. 1st order Sobol index for each parameter  $E_{H1}^0, i_{H1}^0, k_p$  (columns), under each distribution set (rows) detailed in Table 2.

The parameter sensitivities visualized in Fig. 4 highlight the relevance of parameters in different parts of the profiles. It can also be observed that after 3000 seconds, the noise in the Sobol index of  $E^0_{H1}$  and  $i^0_{H1}$  becomes greater, as the variance in output correspondingly decreases significantly (Fig. 3). This can also be observed from Fig. 5 that for all 3 distributions, the variation in state evolution between 3000 -4500 sec becomes small.

The difference in sensitivity magnitude observed in Fig. 4 shows that for distribution set 1 and 2, the parameter  $i_{H1}^0$  remains relatively insignificant. Namely, most of the variance in output during the initial 4000 sec is dominated by  $E_{H1}^0$ . Only in distribution set 3, with a lognormal distribution on parameter  $i_{H1}^0$ , does its sensitivity increase to a detectable level.

Fig. 4 shows that parameter  $k_p$  is the only significant parameter after 4000 sec, in all three distribution sets. This is because  $k_p$  affects the state evolution of  $S^{2-}$  and  $S_p$ , which are only present after 4000 seconds, as seen in Fig. 5. Even though  $k_p$  is the only significant parameter in the later half of the profile, it can be observed that the variance in output caused by  $k_p$  is significantly higher in distribution set 3, as seen in Fig. 3. Fig. 5 further shows the variance in evolution of  $S^{2-}$  and  $S_p$  under different distribution sets. It can be observed that with a much larger parametric range in set 3,  $k_p$  significantly affects the evolution of  $S^{2-}$  and  $S_p$ . This elucidates how different parametric distributions can significantly affect the states, voltage output and its corresponding sensitivity.

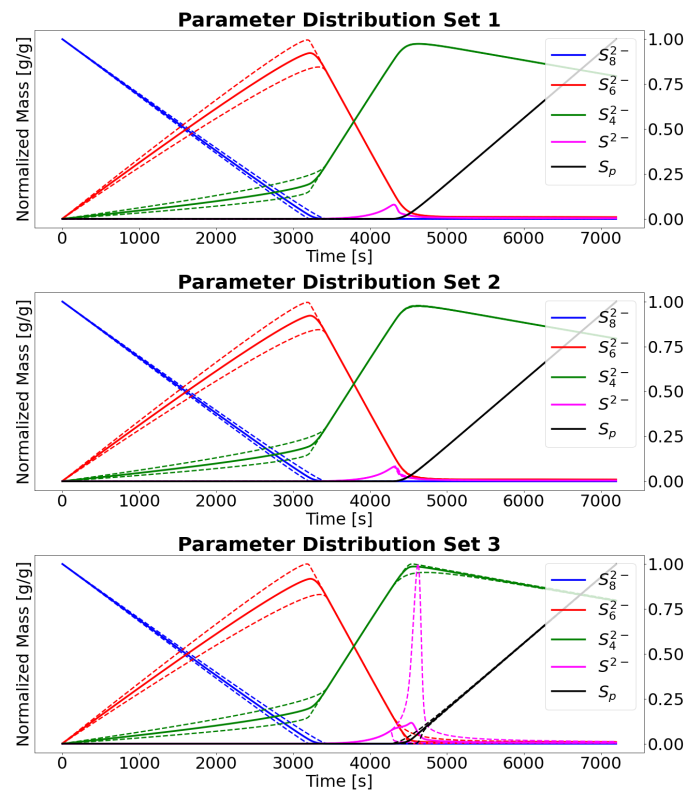


Fig. 5. Evolution of states (mass of sulfur species) for constant current

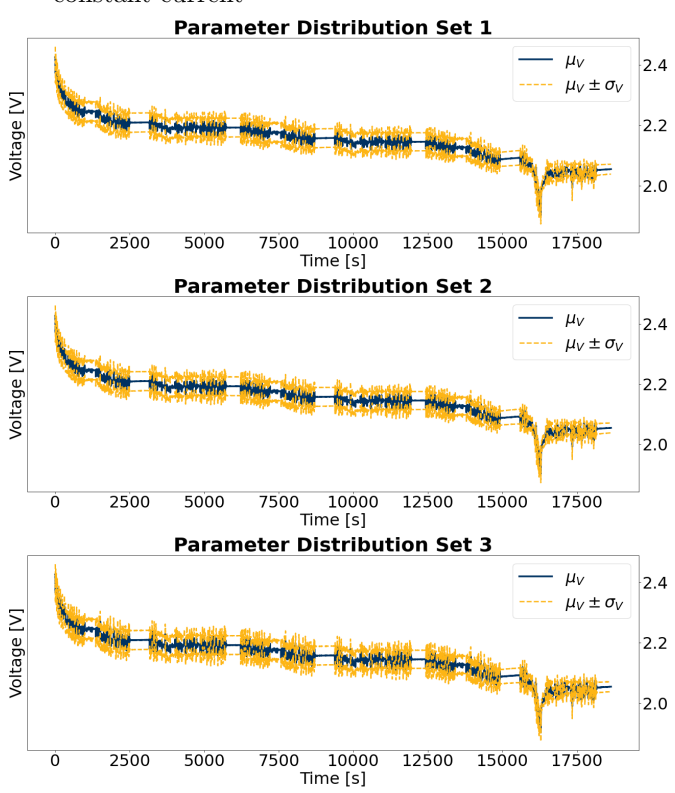


Fig. 6. Voltage for the 3 parameter distributions for dynamic current input.

5.2 Dynamic Cycle Analysis

Next we analyse the sensitivity results for a dynamic input current. For dynamic current we chose a natural-

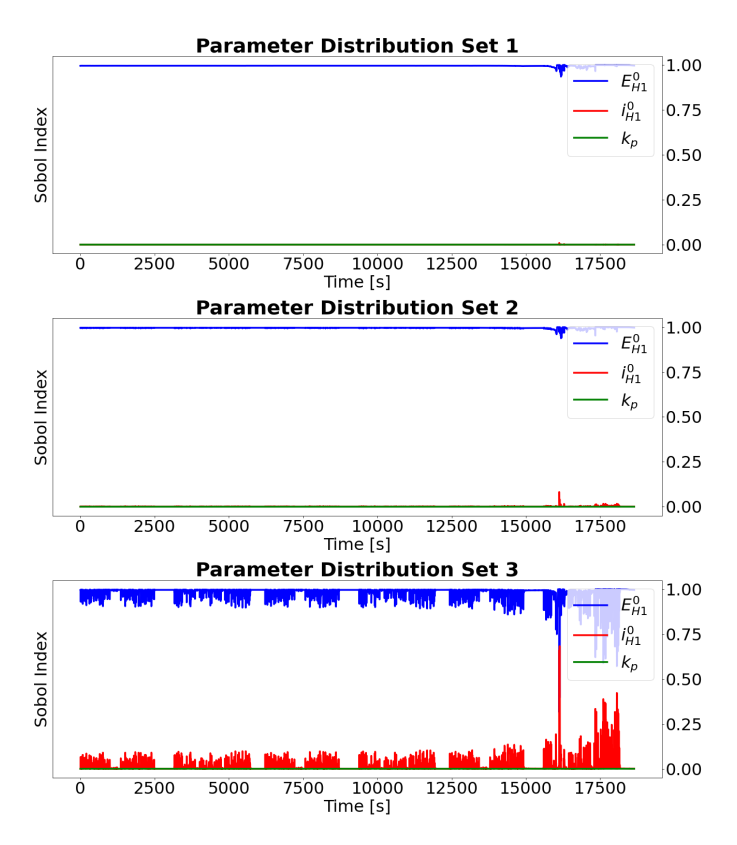


Fig. 7. First order Sobol index for Dynamic current

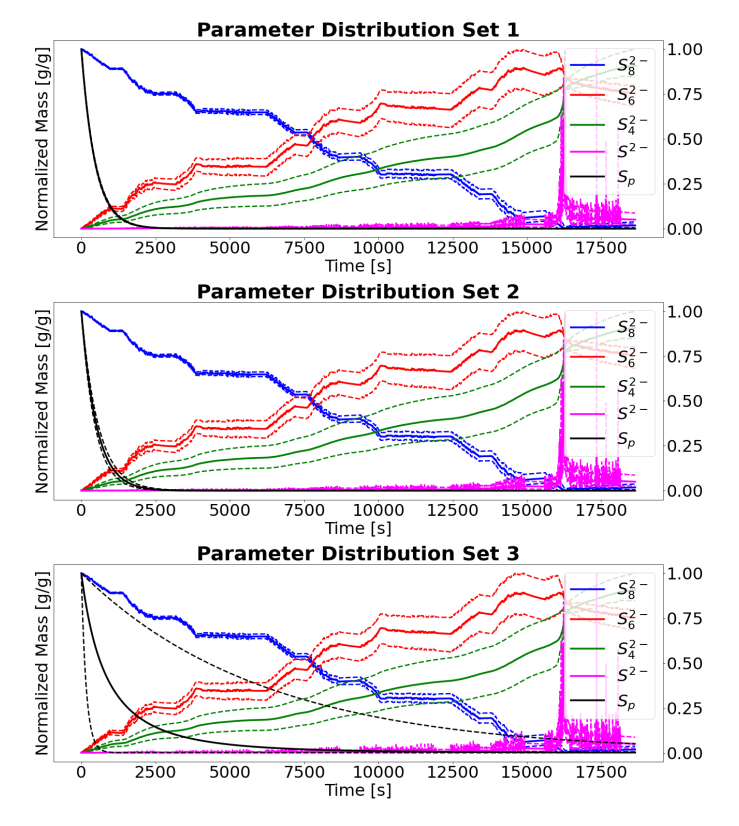


Fig. 8. State evolution s for Dynamic current

istic evening driving cycle (LeBlanc (2006)). We append multiple of this drive cycle to normalize to 2Ah of absolute current throughput. Looking at Fig. 6 and Fig. 8, the distribution of parameters does not have a noticeable impact on the variation on voltage or state trajectories. As such we focus our attention on Fig. 7 which does show a noticeable trend with distribution.

The sensitivity profiles for dynamic current input are displayed in Fig. 7. The most significant parameter in this profile is  $\check{E}^0_{H1},$  across all distribution sets. It can be observed that with increased parametric range for  $i_{H1}^0$ , its sensitivity i.e. variation in voltage caused by  $i_{H1}^0$ increases. For distribution set 3,  $i_{H1}^0$  has a larger sobol index, denoting it becomes a significant parameter. This information is relevant in application, since it implies that  $i_{H_1}^0$  can be a significant if its range of variation is properly chosen. In contrast, even by increasing the range  $k_p$ 's distribution by two orders of magnitude, its sensitivity remains small. This can be explained by looking at the state evolution of species in Fig. 8. Species  $S^{2-}$  and  $S_p$  in most part of the cycle remain minimal, thereby the effect of  $k_p$  on voltage output remains marginal. This implies that for any distribution,  $k_p$  would have very low identifiability for this input profile.

In both the case studies analyzed, it was observed that  $E^0_{H1}$  is a significant parameter across all the distribution sets. However, the significance of parameter  $i^0_{H1}$  and  $k_p$  showed dependency on their distribution. It is also observed that identifiability of parameter greatly depends on the input profile. In case study 1,  $E^0_{H1}$  and  $k_p$  are the parameters significantly affecting voltage response, while  $i^0_{H1}$  remain relatively insignificant, across all distributions. In case study 2,  $i^0_{H1}$  becomes an important parameter, affecting the voltage response (distribution 3), while  $k_p$  remains insignificant.

This analysis advocates for the importance of analyzing parametric sensitivity on proper choice of input profile for parameter identification. It also highlights the effect of proper choice of range of parameter in performing sensitivity analysis.

### 6. CONCLUSION

This paper conducts a meta-analysis on global sensitivity of Li-S model parameters, analyzing its dependence on assumed parameter distributions. Two cases studies are presented, where sensitivities of three parameters are analyzed under three distribution sets. It is observed that information about a parameter a-priori has a significant impact on its relative importance in parameter identification. The input profile as well as the parameter distribution affect the impact a parameter has on voltage response.

This work lays the groundwork for optimal experiment design using GSA. Importantly we highlight the issue that optimal experiments designed using conventional GSA are not robust to the distribution chosen on the parameters. This motivates future work in distributionally robust optimal experiment design.

### ACKNOWLEDGEMENTS

This material is based upon work supported by the National Science Foundation Graduate Research Fellowship Program under Grant No. DGE 2146752. Any opinions, findings, and conclusions or recommendations expressed in this material are those of the author(s) and do not neces sarily reflect the views of the National Science Foundation. This research used the Savio computational cluster resource provided by the Berkeley Research Computing program at the University of California, Berkeley (supported by the UC Berkeley Chancellor, Vice Chancellor for Research, and Chief Information Officer).

### REFERENCES

- Andersson, J.A.E., Gillis, J., Horn, G., Rawlings, J.B., and Diehl, M. (2019). CasADi A software framework for nonlinear optimization and optimal control. *Mathematical Programming Computation*, 11(1), 1–36. doi: 10.1007/s12532-018-0139-4.
- Feng, S., Fu, Z.H., Chen, X., and Zhang, Q. (2022). A review on theoretical models for lithium–sulfur battery cathodes. *InfoMat*, 4(3), e12304.
- Fotouhi, A., Auger, D.J., O'Neill, L., Cleaver, T., and Walus, S. (2017). Lithium-sulfur battery technology readiness and applications—a review. *Energies*, 10(12), 1937.
- Ghaznavi, M. and Chen, P. (2014a). Analysis of a mathematical model of lithium-sulfur cells part iii: electrochemical reaction kinetics, transport properties and charging. *Electrochimica Acta*, 137, 575–585.
- Ghaznavi, M. and Chen, P. (2014b). Sensitivity analysis of a mathematical model of lithium–sulfur cells part i: Applied discharge current and cathode conductivity. *Journal of power sources*, 257, 394–401.
- Guo, Y., Li, H., and Zhai, T. (2017). Reviving lithium-metal anodes for next-generation high-energy batteries. *Advanced materials*, 29(29), 1700007.
- Hou, T.Z., Peng, H.J., Huang, J.Q., Zhang, Q., and Li, B. (2015). The formation of strong-couple interactions between nitrogen-doped graphene and sulfur/lithium (poly) sulfides in lithium-sulfur batteries. 2D Materials, 2(1), 014011.
- Hou, T.Z., Xu, W.T., Chen, X., Peng, H.J., Huang, J.Q., and Zhang, Q. (2017). Lithium bond chemistry in lithium–sulfur batteries. *Angewandte Chemie*, 129(28), 8290–8294.
- Huang, Z., Couto, L.D., Dangwal, C., Xiao, S., Lv, W., Zhang, D., and Moura, S.J. (????). On electrochemical model-based state estimation for lithium-sulfur batteries. ongoing review.
- Iwanaga, T., Usher, W., and Herman, J. (2022). Toward SALib 2.0: Advancing the accessibility and interpretability of global sensitivity analyses. Socio-Environmental Systems Modelling, 4, 18155. doi:10.18174/sesmo.18155. URL https://sesmo.org/article/view/18155.
- Kumaresan, K., Mikhaylik, Y., and White, R.E. (2008). A mathematical model for a lithium–sulfur cell. *Journal of the electrochemical society*, 155(8), A576.
- LeBlanc, D.J. (2006). Road departure crash warning system field operational test: methodology and results. volume 1: technical report. Technical report, Univer-

- sity of Michigan, Ann Arbor, Transportation Research Institute.
- Lim, W.G., Kim, S., Jo, C., and Lee, J. (2019). A comprehensive review of materials with catalytic effects in li–s batteries: enhanced redox kinetics. *Angewandte Chemie*, 131(52), 18920–18931.
- Liu, D., Zhang, C., Zhou, G., Lv, W., Ling, G., Zhi, L., and Yang, Q.H. (2018). Catalytic effects in lithium-sulfur batteries: promoted sulfur transformation and reduced shuttle effect. Advanced Science, 5(1), 1700270.
- Marinescu, M., Zhang, T., and Offer, G.J. (2016). A zero dimensional model of lithium–sulfur batteries during charge and discharge. *Physical Chemistry Chemical Physics*, 18(1), 584–593.
- Park, S., Kato, D., Gima, Z., Klein, R., and Moura, S. (2018). Optimal experimental design for parameterization of an electrochemical lithium-ion battery model. *Journal of The Electrochemical Society*, 165(7), A1309.
- Parke, C.D., Subramaniam, A., Kolluri, S., Schwartz, D.T., and Subramanian, V.R. (2020). An efficient electrochemical tanks-in-series model for lithium sulfur batteries. *Journal of The Electrochemical Society*, 167(16), 163503.
- Parke, C.D., Teo, L., Schwartz, D.T., and Subramanian, V.R. (2021). Progress on continuum modeling of lithium–sulfur batteries. Sustainable Energy & Fuels, 5(23), 5946–5966.
- Peng, L., Wei, Z., Wan, C., Li, J., Chen, Z., Zhu, D.,
  Baumann, D., Liu, H., Allen, C.S., Xu, X., et al. (2020).
  A fundamental look at electrocatalytic sulfur reduction reaction. *Nature Catalysis*, 3(9), 762–770.
- Ramancha, M.K., Astroza, R., Madarshahian, R., and Conte, J.P. (2022). Bayesian updating and identifiability assessment of nonlinear finite element models. *Mechanical Systems and Signal Processing*, 167, 108517.
- Saltelli, A., Annoni, P., Azzini, I., Campolongo, F., Ratto, M., and Tarantola, S. (2010). Variance based sensitivity analysis of model output. design and estimator for the total sensitivity index. Computer physics communications, 181(2), 259–270.
- Saltelli, A., Ratto, M., Andres, T., Campolongo, F., Cariboni, J., Gatelli, D., Saisana, M., and Tarantola, S. (2008). Global sensitivity analysis: the primer. John Wiley & Sons.
- Wang, S., Feng, S., Liang, J., Su, Q., Zhao, F., Song, H., Zheng, M., Sun, Q., Song, Z., Jia, X., et al. (2021). Insight into mos2-mon heterostructure to accelerate polysulfide conversion toward high-energy-density lithiumsulfur batteries. Advanced Energy Materials, 11(11), 2003314.
- Xu, C., Cleary, T., Li, G., Wang, D., and Fathy, H. (2021). Parameter identification and sensitivity analysis for zero-dimensional physics-based lithium-sulfur battery models. ASME Letters in Dynamic Systems and Control, 1(4).